HHS Public Access

Author manuscript

Neuromodulation. Author manuscript; available in PMC 2024 June 09.

Published in final edited form as:

Neuromodulation. 2024 June ; 27(4): 625–635. doi:10.1016/j.neurom.2022.11.009.

Forward Stepping Evoked by Transvertebral Stimulation in the Decerebrate Cat

Vsevolod Lyakhovetskii, PhD[1,a], **Polina Shkorbatova, PhD**[1,2,3,a], **Oleg Gorskii, MS**[1,2], **Pavel Musienko, MD, PhD**[1,2,4]

[1]Pavlov Institute of Physiology Russian Academy of Sciences, St Petersburg, Russia

[2]Institute of Translational Biomedicine, Saint Petersburg State University, St Petersburg, Russia

[3]Department of Neurobiology, Sirius University, Sirius, Sochi, Russia

[4]National University of Science and Technology “MISIS,” Moscow, Russia

Abstract

Objectives: Implantation of stimulating electrodes into the basement of the vertebral spinous process allows the electrodes to be quickly and stably fixed relative to the spinal cord. Using this approach, we have previously shown the selectivity of rat muscle activation during transvertebral stimulation (TS). In this work, we investigated the TS to induce forward stepping of the cat’s hindlimbs in comparison with epidural stimulation (ES).

Materials and Methods: TS was performed with an electrode placed in the VL3–VL6 vertebrae in five decerebrated cats. ES was performed on the same cats in L5–L7 segments. Kinematic parameters of stepping were recorded in addition to electromyographic activity of musculus (m.) iliopsoas (IP), m. tibialis anterior (TA), and m. gastrocnemius lateralis (GL) of both hindlimbs.

Results: With VL3–VL4 TS, all five animals were capable of bipedal forward stepping, whereas VL5 and VL6 TS led to the forward stepping in 3 of 5 and 1 of 5 animals, respectively. Well-coordinated muscle activity led to a high level of intra- and interlimb coordination. Kinematic parameters of TS-induced stepping were similar to those obtained with ES. The TS of the VL3 vertebra causes the frequency lock with the integer multiple of the stimulation frequency. Similarly to the rat model, TS-evoked muscle responses were site specific. They were minimal during VL3 TS and were maximal during VL4–VL5 TS (IP) and VL5–VL6 TS (TA, GL).

Address correspondence to: Pavel Musienko, MD, PhD, Pavlov Institute of Physiology Russian Academy of Sciences, Makarov emb, 6, St Petersburg, Russia 199034. pol-spb@mail.ru.

[a]Indicates equal contribution.

Authorship Statements

Polina Shkorbatova, Vsevolod Lyakhovetskii, Oleg Gorskii, and Pavel Musienko conceived and performed the experiments. Polina Shkorbatova and Vsevolod Lyakhovetskii analyzed the data. Polina Shkorbatova, Vsevolod Lyakhovetskii, and Oleg Gorskii wrote the manuscript. Vsevolod Lyakhovetskii created the figures. Polina Shkorbatova, Oleg Gorskii, and Pavel Musienko edited the manuscript. Pavel Musienko supervised the study. All authors contributed to the article and approved the submitted version.

SUPPLEMENTARY DATA

To access the supplementary material accompanying this article, visit the online version of *Neuromodulation: Technology at the Neural Interface* at www.neuromodulationjournal.org and at https://doi.org/10.1016/j.neurom.2022.11.009.

Conflict of Interest: The authors reported no conflict of interest.

Conclusions: The obtained results support hypotheses about the location of the central pattern generators in the upper lumbar spinal segments. The proposed approach of electrode placement is surgically easier to perform than is ES. This approach is useful for studying site-specific neuromodulation of the spinal sensorimotor networks and for investigating new strategies of locomotor recovery in animal models.

Keywords

Central pattern generators; decerebrate cat; locomotion; spinal cord; transvertebral stimulation

INTRODUCTION

Locomotion is a crucial ability of all animals and humans. The loss of this essential function dramatically impairs the quality of life in patients with spinal cord injuries.[1,2] Such injuries partly or totally isolate the spinal cord neuronal circuitries from supraspinal control, resulting in complete or partial paralysis of the lower extremities[3] and multiple dysfunctions of the pelvic organs.[4] A large body of work is dedicated to the different techniques of exogenous modulation of the activity of these circuitries to find suitable methods for locomotor recovery.[5]

In acute or chronic experiments, the locomotion may be elicited in different animal models (intact, spinalized, or decerebrate) by many techniques such as forelimb facilitation,[6] perineal stimulation,[7] and tail pinching,[8] in addition to chemical,[9] magnetic,[10] and electrical stimulation.[11–17] Electrical stimulation is a popular method to activate spinal locomotor networks that is used in animal models and as a part of locomotor neurorehabilitation training after injuries in humans. Such training is still in the experimental stage but gives promising results to gait restoration.[18,19] Electrical stimulation is delivered by an electrode placed in different anatomic regions. In animals, the electrode may be placed in some brainstem areas,[11] inside the spinal cord,[7] on the dorsal roots,[7,12] subdurally,[13] epidurally,[13–16] or subcutaneously.[17] In humans, for restoration after spinal cord injuries, stimulation may be delivered epidurally[18] or transcutaneously.[19] The latter approach is noninvasive; thus, it can be used even in healthy subjects to study the peculiarities of locomotion.[20]

The hairy and easily movable skin surface of an animal makes the stable cutaneous electrode fixation difficult.[21,22] In addition, animals possess cutaneous trunk muscles, which easily move in response to skin stimulation or in normal animal behavior.[23] Presumably, an unstable electrode position decreases the quality of transcutaneously induced locomotion, making it less coordinated and more unstable than locomotion induced by epidural stimulation (ES).[21] Therefore, transcutaneous stimulation is rarely used in animal models in locomotor studies, though such stimulation can initiate locomotor activity in acute decerebrate[21] and chronic spinal cats.[21,24] However, thus far, transcutaneous stimulation has been used in experiments on animals conducted under general anesthesia (studies of evoked potentials on leg muscles,[22] studies of neuropathic pain,[25] and studies of activation of lower urinary tract[26]) in which the animals are unconscious and unable to displace or remove the stimulation electrode.

Previously, we proposed a compromise approach for electrode implantation in vertebral spinous processes. Vertebral implantation is faster (Surgery and Stimulation Procedures section provides the timeline) and less invasive than epidural implantation, and an electrode may be placed more stably than for the transcutaneous stimulation. Using this technique, we revealed the site specificity of the sensorimotor spinal network in decerebrate rats by the muscle evoked potential method.[27] The preliminary results have shown that transvertebral stimulation (TS) may also initiate the forward walking (FW) of decerebrate rats.[28] However, the decerebrate rats possess a high level of spontaneous activity,[29] and they often react unpredictably to different external stimuli,[30] making it difficult to receive stable locomotion in response to electrical spinal cord stimulation. The recently developed decerebrate mouse model[31] to study locomotion has not been tested for the possibility of walking initiated by electrical stimulation.

Since Sherrington's work,[32] cats have been widely used in locomotor studies.[8,33] The decerebrated model allows us to elicit stable and well-coordinated locomotion by electrical stimulation of the lumbar spinal cord in acute experiments in comparison with the spinal model.[34] The same model, in contrast to the intact one, allows us to explore the locomotor automatism depending primarily on the spinal networks. The importance of studying these networks in animal models is that spinal circuits are the targets of different methods of posttraumatic gait restoration in humans.[35] The decerebrate model has been extensively used to study the spinal neural circuits of backward and bidirectional locomotion on split-belt treadmill and the supraspinal control of these rather unusual locomotor modes.[14–16] This study aims to investigate the FW of decerebrate cats elicited by TS and to compare its quality with the FW elicited by ES. We hypothesize that TS site specifically activates the locomotor neuronal circuitries located in the lumbar spinal cord in decerebrate cats.

MATERIALS AND METHODS

Animals

Five normally pigmented adult cats (all females), weighing 2.5 to 4 kg, were used for the experiments. The animals were bred and housed at the animal facility of the Pavlov Institute of Physiology. All experimental procedures were performed in accordance with a protocol approved by the Animal Care Committee of the Pavlov Institute of Physiology, St Petersburg, Russia, and followed the European Community Council Directive (2010/63EU) and the guidelines of the National Institutes of Health Guide for the Use of Laboratory Animals, Animal Welfare Assurance #A5952–0.

Surgery and Stimulation Procedures

The animals were anesthetized with isoflurane (4%–5% for induction, 2%–2.5% for maintenance), mixed with oxygen (flow rate 0.8 L/min) and decerebrated at precollicular–postmammilar level, as described earlier.[15] The anesthesia was discontinued after the decerebration. Stainless steel bipolar wire electrodes (AS632, Cooner Wire, Chatsworth, CA) were implanted bilaterally into the iliopsoas (IP), tibialis anterior (TA), and gastrocnemius lateralis (GL) muscles to record the electromyographic activity (EMG) during FW and evoked potential recording. The head, vertebral column, and pelvis of the animal

were fixed in a rigid frame. The hindlimbs of the animal were placed on a treadmill (Fig. 1a); the distance between the treadmill belt and animal pelvis was 21 to 25 cm (depending on the animal's size). Next, the skin and paravertebral muscles were opened, and the spinous processes of the vertebrae VL2–VL6 were removed with a Luer bone rongeur. The experiment started after 1.5 to 2 hours, when the animal was fully recovered from anesthesia. A custom-made electrode prepared from a 23G needle covered by plastic insulation with a 1.5 mm uninsulated tip was used for TS and placed alternately in the basement of the spinous process of the vertebrae VL2–VL6 (Fig. 1b). Thus, the process of inserting the transvertebral electrode took 2 to 3 minutes. The ground electrode was placed under the abdomen skin in the midline area. To record the muscle evoked potentials, the following parameters of electrical stimulation were used: single impulses with 1 Hz frequency, 0.2- to 0.3-millisecond impulse duration, and 100- to 3500-μA current amplitude. To elicit locomotion, we used biphasic impulses with 3- to 5-Hz frequency and 0.2- to 0.3-millisecond pulse duration; the current amplitude was gradually increased starting from 100 μA. This increase was stopped when the stable alternating locomotor limb movements were clearly seen (100–3000 μA) or the amplitude of rhythmical synchronous twitching of both hindlimbs became extremely large. Then, the laminectomy of the caudal part of VL4 and the rostral part of VL5 was performed to provide access to the L5–L7 spinal cord segments (timing approximately 15–20 minutes). Then we searched for the stimulation point with the optimal stepping parameters by moving the electrode rostrally or caudally inside the laminectomy (timing approximately 2–10 minutes). To elicit locomotion, a monopolar silver ball electrode (diameter = 0.5 mm) was positioned on the dura mater of the spinal cord dorsal surface, and the following parameters of ES were used: 5-Hz frequency, biphasic mode, 0.2- to 0.3-millisecond pulse duration, and 20- to 130-μA current intensity. Similarly to TS, current amplitude increased from 10 μA until stable locomotion was obtained. To record the muscle evoked potentials, the following parameters of ES were used: single impulses with 1-Hz frequency, 0.2-millisecond biphasic impulse duration, and 10- to 120-μA current amplitude.

For each animal, one test of evoked potentials and one locomotor test were performed at each stimulation point. Ten evoked responses were recorded at each stimulation current. At least ten successive steps of each hindlimb were performed if alternating locomotor limb movements were clearly seen.

At the end of the experiment, the animal was euthanized with an overdose of isoflurane (5% mixed with oxygen, flow rate 1 L/min). A careful dissection was then performed to determine the exact segment of stimulation based on dorsal roots emerging from the spinal cord.[36]

Data Analysis

Locomotion

Most studied parameters have been previously introduced.[14–16] Briefly, ground reaction forces (GRFs) were recorded by strain gauges located under the treadmill belts; two mechanical sensors were attached to the ankles to record rostrocaudal hindlimb movements. The step length, period of stepping, and duration of stance and swing phases were

derived from the trajectories of these movements. The Pearson correlation coefficient was assessed for the trajectories of hindlimb movements. With coordinated forward stepping, the trajectories of movement of the limbs were almost in the antiphase, resulting in a strongly negative cross-correlation coefficient.[16]

The individual steps of more stable locomotion are more similar to each other than are the steps of less stable and less coordinated locomotion. Thus, the trajectory of more stable stepping (solid line) will be more similar to itself when shifted by a step period than to the trajectory of less stable stepping (dotted line), resulting in a higher value of the second peak of the autocorrelation function. The rostrocaudal stability was calculated as the value of the second peak of the autocorrelation function of the hindlimb trajectory (because the first peak of the autocorrelation function is always equal to 1, Fig. 1e).[14–16] The asymmetry of stepping periods was estimated as the ratio of the module difference between the period of neighboring steps of the left (T_{left}) and right (T_{right}) hindlimbs to their sum,[14,16] ie,

$$\frac{|T_{left} - T_{right}|}{T_{left} + T_{right}}$$

The proximity of the stepping period to a multiple of the stimulation period[37] was determined as

$$\min(T_{stepping} \; mod \; T_{stim}, \; T_{stim} - T_{stepping} \; mod \; T_{stim})$$

where *mod* is the modulo operation, $T_{stepping}$ is the animal stepping period, and T_{stim} is the stimulation period (200 milliseconds or 333 milliseconds). If $T_{stepping}$ is almost equal to a multiple of T_{stim} (Fig. 1d, solid line), the swing-stance transition points are located in the same way in relation to TS pulses (to the left compared with the nearest stimulation pulse). If $T_{stepping}$ is less proximal to the multiple of T_{stim} (dotted line), the swing-stance transition points are located differently in relation to TS pulses (to the left or right compared with the nearest stimulation pulse). These three stepping characteristics are unit free.

The angle range in the hip, knee, and ankle joints (ie, the difference of the minimal angle during the swing phase and the maximal angle during the stance phase in the given joint [Fig. 1c]) was calculated based on the manual analysis of video records (50 frames/s) containing the positions of light-reflective markers placed on the iliac crest, greater trochanter of the femur, lateral condyle of the femur, and lateral malleolus.

EMG signals were normalized to their integral value in a step cycle during ES on a per animal basis. The signals of EMG, GRFs, and mechanical sensors were amplified and digitized at 20 kHz with an A/D board (LTR-EU-16, LTR11, L-Card, Moscow, Russia), and EMG signals were further filtered in 100- to 2000-Hz bandwidth.

Rostrocaudal stability was calculated for all steps (because the autocorrelation function needs several periods of signal to be calculated), whereas other characteristics were calculated for each step and then averaged over all steps.

Evoked Potentials—The analysis of muscle evoked potentials was performed similarly to Havton et al., 2019.[26] The window to select the components of evoked potential was taken as 1 to 20 milliseconds after the stimulation impulse. The sensory and motor components of evoked potentials were separated manually by an expert on the basis of their latency and their order of appearance at current increase (the sensory component emerges at lower current) (Fig. 1f). For each muscle of each animal, the recruitment curves of peak-to-peak amplitude (average of ten responses at each current) were plotted separately for motor and sensory components of potentials evoked by stimulation of the VL3–VL6 vertebrae. The slopes of the ascending part of these curves were assessed (Fig. 1g,h). For each muscle, the slopes ($Slope_i$, i = VL3…VL6) were normalized to the maximal slope within the given muscle of the given animal ($Slope_{max}$). Next, the averaged normalized slopes were obtained. Presumably, such slope distributions qualitatively reflect the distribution of motoneuronal pools in spinal segments.[38] The latencies of early and medium responses and their threshold currents (current at which peak-to-peak response amplitude exceeds 0.01 mV) were measured for vertebrae whose stimulation elicited the recruitment curves with the maximal slope.

Statistical Analysis

A single hindlimb (either left or right) was used as an experimental unit for all tests of intralimb coordination ($n = 10$) because the significant differences between temporospatial stepping characteristics of the left and right hindlimb of the intact cat are absent;[39] a single animal was used as an experimental unit for all tests of interlimb coordination ($n = 5$). The data are presented as the mean ± SD. To compare the muscle activity, its integral EMG value was taken in bins where the muscle was active. The Friedman test with post hoc Dunn's multiple comparison test was used to determine the significance of the differences between individual pairs of means when comparing three groups. The Wilcoxon matched-pairs signed-rank test was used to determine the significance of the differences between individual pairs of means when comparing two groups. A p value of 0.05 was used as the cutoff for significance. Statistical calculations were performed using Prism 7.0 (GraphPad Software, La Jolla, CA).

RESULTS

Forward Walking

Different animals can FW during stimulation of different vertebrae and during ES; the segment of ES and the current needed to initiate FW are listed in Table 1. Only one animal was able to FW during VL6 stimulation; another animal was able to FW during VL2 stimulation; three animals were able to FW during VL5 stimulation, whereas all five animals were able to FW during VL3, VL4 stimulation, and ES (Fig. 2a; Supplementary Data Video S1). Thus, we will focus mainly on the comparison of features of locomotion elicited in the last three modes.

The representative example of responses of IP, TA, and GL muscles of both hindlimbs and their GRFs, in addition to hindlimb trajectories during FW elicited by VL3 stimulation, is

shown in Figure 3 (left plate). The flexors (TA, IP) are active in the swing phase of hindlimb stepping, whereas the extensors (GL) are active in the stance phase.

Similar muscle activation patterns result in the similar rostrocaudal stability of hindlimb movement, which is the self-similarity of hindlimb trajectories (Fig. 2c, Table 2). Independently of stimulation mode, FW shares similar angle range between maximal flexion and maximal extension in the hip, knee, and ankle joints (Fig. 2 d–f, Table 2). In turn, similar angle ranges in these joints lead to similar step length irrespective of stimulation mode (Fig. 2b , Table 2).

The flexors and extensors of both hindlimbs act reciprocally during VL3 and VL4 TS, which leads to a stable pattern of coordinated FW accompanied by substantial pressure on treadmill belts (Fig. 3). The hindlimbs move in almost antiphase in coordinated FW (ie, one hindlimb moves forward in its swing phase, whereas the other one moves backward in its stance phase). Thus, the trajectory correlation of hindlimbs is strongly negative to all three locomotor modes (Fig. 2g, Table 2). Such coordinated FW is also characterized by low time asymmetry, which is the weighted difference between the stepping period of both hindlimbs (Fig. 2h, Table 2).

However, the relative amplitude of EMG activity of the muscles of both hindlimbs considered depends on the stimulation mode (Fig. 4). IP is more active during ES relative to VL3 ($p = 0.02$) and VL4 ($p = 0.03$) stimulation [FM(3) = 9.25, $p = 0.008$]. TA and GL are more active during ES relative to VL3 (both, p = 0.005) stimulation [FM(3) = 9.8, $p = 0.0063$ and FM(3) = 10.4, $p = 0.0034$, respectively]. GRFs arising during ES in the stance phase of FW are significantly higher than those in VL3 ($p = 0.0024$) and VL4 ($p = 0.0024$) stimulation [FM(3) = 15, $p = 0.0001$] (Fig. 4).

Although the kinematic parameters of the FW elicited in different stimulation modes remain similar, its temporal characteristics possess some peculiarities. The period of stepping differs between three modes of stimulation; specifically, the period for VL4 stimulation is higher than that for ES ($p = 0.01$) (Fig. 2j, Table 2). The relative durations of swing and stance phases are not significantly different (Fig. 2k,l, Table 2). At the same time, the stepping periods have a different level of proximity to a multiple of the stimulation period, ie, the proximity to 800 milliseconds (4 × 0.2 seconds in case of 5-Hz stimulation) or 660 milliseconds (2 × 0.33 seconds in case of 3-Hz stimulation). The period of FW during VL3 stimulation is more proximal to a multiple of the stimulation period relative to VL4 stimulation ($p = 0.0024$) and ES ($p = 0.0024$) (Fig. 2i, Table 2).

Evoked Potentials

In four of five animals, the stimulation of VL6 led only to the rhythmical synchronous twitching of both hindlimbs (Fig. 3, right plate). To reveal the potential reasons for the absence of locomotion during stimulation of the lower lumbar vertebrae, we performed the mapping of the spinal sensorimotor network by the muscle evoked potential method. The representative example of analysis of the evoked potentials of the right IP is shown in Figure 5a–c. It is observed that the sensory (medium) component of responses appeared at lower current amplitude during VL5 stimulation. Its peak-to-peak amplitude decreased

with increasing current amplitude, whereas the amplitude of the motor (early) responses increased. During the stimulation of VL4 with the same current, the amplitude of all components of evoked potentials is much lower (Fig. 5a). During TS of VL3 and VL6, the amplitude of all components of evoked potentials is very small relative to TS of VL5. Only the sensory component of response appeared during the ES of L6 segment. The peak-to-peak amplitude of early and medium responses was used separately to build the recruitment curves (Fig. 5b,c).

The latencies and threshold currents were estimated for each muscle of both hindlimbs during the stimulation of the vertebra in which the slope of the recruitment curve of early responses was maximal (IP: VL4 [$n = 3$] and VL5 [$n = 7$], TA: VL5 [$n = 5$] and VL6 [$n = 5$], GL: VL5 [$n = 4$] and VL6 [$n = 6$]). The latencies of early responses during stimulation in optimal for particular muscle vertebrae are significantly different; that is, the latency of IP early response is lower than that of GL ($p = 0.02$) and TA ($p < 0.001$). The latencies of medium responses are also significantly different; ie, the latency of IP medium response is lower than that of GL ($p = 0.028$) (Fig. 5d, Table 3). Meanwhile, threshold currents of early responses during stimulation in optimal for particular muscle vertebrae are similar; the same results are obtained for threshold currents of medium responses (Fig. 5e, Table 3). At this time, threshold currents of medium responses are lower than those of early responses [tendencies for IP and GL currents: $W(10) = 16$, $p = 0.16$ and $W(10) = 19$, $p = 0.14$, respectively; significant difference for TA currents: $W(10) = 36$, $p = 0.0078$]. The average distributions of the normalized slopes vs the mean skeletotopy of the VL3–VL6 region for early and medium responses are shown in Figure 5f–h. All average distributions of normalized slopes for early and medium components of evoked potentials have minimal values during VL3 stimulation (Fig. 5g,h). Meanwhile, during VL6 stimulation, the slopes of recruitment curves are different for early [$FM(3) = 15.66$, $p = 0.0004$] and medium [$FM(3) = 13.69$, $p = 0.0011$] components; that is, the slope of IP response components is lower than that of GL ($p = 0.0005$ and $p = 0.0009$ for early and medium component, respectively) and TA ($p = 0.0048$ and $p = 0.018$ for early and medium component, respectively).

DISCUSSION

The use of a well-established animal model, that is, decerebrate cat, allowed us to compare reliably different types of spinal cord electrical stimulation. All cats used in the study were capable of coordinated bipedal FW with high intra- and interlimb coordination and kinematic parameters induced by VL3–VL4 TS, similar to those obtained with ES. High stability of locomotion was obtained owing to reciprocal burst activity of ipsilateral antagonist muscles and bilateral alternation of burst activity of synergistic muscles. Thus, the proposed approach significantly expands the possibilities of studying FW in animal models. Surgical access with implantation of electrodes for electrical stimulation in the spinous processes of the vertebrae is simple and inflicts minimal trauma because it misses the laminectomy — a quite invasive, time-consuming, and high-risk procedure which requires sufficient skill of the surgeon.[40,41] Using these electrode positions, the motor activity is initiated minimally invasively without performing laminectomy and complicated surgical implantation of electrodes and subsequent laborious medical care; in addition, there

are no risks associated with an implanted electrode on the surface of the spinal cord. TS can be used in movement physiology to study the neuronal control of posture and locomotion at spinal level, in addition to, after further technologic improvement, in clinical medicine for minimally invasive methods of neuromodulation and rehabilitation after vertebro-spinal injury.[42]

The revealed difference between stepping periods can be explained by primary activation of the different circuits of the rhythmogenic level of the central pattern generator (CPG).[43,44] ES, in addition to brainstem stimulation, is performed at frequencies higher than the frequency of typical FW (in decerebrate cat, these frequencies are 3–5 Hz for ES and 30–40 Hz for brainstem stimulation vs 0.6–1.6 Hz for FW). Thus, the frequency of the coordinated FW is independent of the frequency of the ES that elicits locomotion.[45] Our study shows that the frequency of the FW is also independent of the integer multiple of the frequency of L5–L7 spinal segments ES. Meanwhile, decerebrate cats often performed one step for each impulse of dorsal root stimulation, or their stepping period had a complex association with that of stimulation.[12] The frequency of trains of intraspinal microstimulation (0.65–1 Hz) was matched with the frequency of locomotor cycles in seven of 11 cats.[7] Interestingly, the frequency lock observed in the work of Barthélemy[7] occurred during the intraspinal microstimulation of middle L3 or rostral L4 segments. In our study, the TS of VL3 vertebra causes the frequency lock not with the stimulation frequency but with its integer multiple. The frequency lock with the integer multiple of stimulation frequency was also observed in the stepping of children with paraplegia during ES.[37]

It is generally accepted that the essential parts of CPG are located in the rostral part of the lumbar spinal cord, that is, in L3–L4 segments in acute[9] and chronic[46] spinal cats and in L2 level in the spinal rat[47] Meanwhile, the whole lumbar enlargement possesses rhythmogenic ability.[48] Even the caudal lumbar spinal cord is able to initiate locomotion; that is, the ES of lumbar enlargement (L5–S1) evokes locomotor-like EMG activity in chronic spinal cats;[49] the chronically isolated lumbar half spinal cord (below L4) generates activity in the ipsilateral hindlimb of the cat.[50] Our results are in line with the point of view that the rhythmogenic networks of the multilevel CPG[44] are located in the L3–L4 spinal cord region if we assume that TS is predominantly site specific; that is, the VL3–VL4 stimulation leads to activation of L3–L4 spinal networks. Similarly to transcutaneous stimulation, this specificity may be due to activation of the ventral and dorsal roots.[51]

To check the site specificity, we used the evoked potentials from the same loci (ie, from the same vertebra entrance/exit for the FW), which is the method that has previously shown the site specificity of muscle activation by TS in decerebrate rats.[27] The muscle responses to TS consisting of sensory and motor components are similar to those to transcutaneous stimulation of the spinal cord of decerebrate cats but not to those to ES when the motor component is absent (Fig. 5a [21]). The threshold current of sensory components of these evoked potentials is lower than that of the motor one. An increase in the amplitude of the motor component of the response leads to a decrease in the amplitude of the sensory components. The latencies of early and medium responses of IP muscle, which is located more proximally to the stimulation loci (and the nerve carrying the impulses from the spinal cord to the muscle is shorter) than are GL and TA, are the lowest. The largest responses of

TA and GL, whose motoneurons are distributed in the lower lumbar spinal cord,[38] appear during VL6 (inside which the sacral segments of spinal cord are located) stimulation but not during VL5 (inside which the lower lumbar segments are located) stimulation (Fig. 5f [36]). Thus, we confirmed that the targets of the TS are both the dorsal and ventral roots of the segment eponymous to the stimulated vertebra in their entrance/exit from the vertebral canal.[27] As a result of this site specificity, the obtained distribution of average normalized slopes is qualitatively similar to the distribution of the IP, GL, and TA motoneurons.[38] The potentials evoked by VL3 and VL4 stimulation are weak relative to those of VL5 and VL6 stimulation. In contrast, the chances of eliciting locomotion are the highest for VL3 and VL4 stimulation. Thus, similarly to ES, the transvertebrally elicited locomotion is induced presumably not by stimulation of motoneuronal pools by themselves but by transsynaptically activated CPG circuits.[52]

Presumably, the higher GRFs and EMG amplitudes during ES can be explained by several factors. First, TS single pulses evoke the motor component of muscle response at a submaximal current contrary to ES.[21] Thus, the direct activation of motor axons may also appear during TS stepping initiation. This activation partly inhibits medium and late muscle responses and weakens muscle activation. Second, the ES point is nearer to the dorsal L5–L7 roots forming the sensory pathways to TA and GL motoneurons, and to the dorsal L4–L5 roots forming the sensory pathways to IP motoneurons at their entrance to the spinal canal.[14] Third, during TS, the current spreads more widely, activating not only the spinal roots but also directly activating the muscles surrounding the vertebra. This undesirable muscle contraction does not let us increase current further to possibly reach better quality of walking. However, despite a relatively narrow range of current intensities that we can use in TS, we were still able to produce well-coordinated and stable locomotion, comparable with ES-evoked locomotion in kinematic parameters.

Limitations

Although the TS through the needle placed in the spinous process[53,54] or through pedicle screws[55,56] is used in clinical practice for assessment of the functional state of the spinal cord during spinal surgery, the TS proposed in this study to initiate locomotion is still an experimental technique. The method has been approved in acute decerebrate preparation to induce well-coordinated locomotion, but it has not yet been tested in chronic animal models of spinal cord injury.

For cats, the stimulation amplitude of TS is lower than the amplitude used for the transcutaneous one (10–100 mA[21]) and is one order of magnitude higher than that for ES (Table 1) because the vertebral electrode is much further from the spinal cord than is the epidural one. Additional tissues, particularly the structures of the spine and muscles, appear in the path of the stimulation current. This can be attributed to the limitations of the vertebral stimulation method, and to those of the transcutaneous one, which results in less site-specific stimulation effects than does the more invasive ES method.

In addition, one of the limitations of the TS application may be a congenital abnormality of animal vertebral structure. For example, in cats with other than C7T13L7S3 vertebral formula, we cannot predict the optimal vertebra for TS because there are no anatomical data

on spinal segment positions inside the vertebral column in these animals. The application of the TS in our study was also limited to the lumbar vertebrae VL2–VL6 and did not extend to other parts of the spine, among which the cervical spine is of the greatest interest because ES of the cervical enlargement has shown its efficacy at eliciting locomotion.[13]

All animals used in the study were females. Although we know that the main stepping parameters (vertical force, gait cycle time, stance time, and swing time) are reported to not significantly differ between male and female cats (except the step length, which is larger for males[39]), and the positions of the spinal cord segments also do not differ between males and females,[57] the use of one sex should be regarded as a limitation of the study. However, if one uses TS to modulate the functions of pelvic organs, sex may have a significant influence.

CONCLUSIONS

The presence of locomotion during the TS of vertebrae, whose eponymous segments do not contain motoneuronal pools, supports hypotheses about the location of the CPGs in the upper lumbar segments of the spinal cord. The developed model is useful for studying the mechanisms of neuromodulation of the sensorimotor networks of the spinal cord and for investigating new approaches of neurorehabilitation after spinal cord and brain injury and diseases.

Supplementary Material

Refer to Web version on PubMed Central for supplementary material.

Source(s) of financial support:

This work was performed within project ID: 73025408/93022798 of the St Petersburg State University, St Petersburg, Russia (for Polina Shkorbatova and Oleg Gorskii) and by the Ministry of Science and Higher Education of the Russian Federation under the strategic academic leadership program “Priority 2030” (for Pavel Musienko), supported by Russian Science Foundation Grant 21-15-00235 (for electrophysiological testing) and Grant 22-15-00092 (for developing the stimulating method), National Institutes of Health Grant R01 NS-100928 (for developing the experimental setup), and by Sirius University, project number NRB-RND2115 (experimental surgery).

REFERENCES

1. Westgren N, Levi R. Quality of life and traumatic spinal cord injury. Arch Phys Med Rehabil. 1998;79:1433–1439. 10.1016/s0003-9993(98)90240-4. [PubMed: 9821906]
2. Anderson KD. Targeting recovery: priorities of the spinal cord-injured population. J Neurotrauma. 2004;21:1371–1383. 10.1089/neu.2004.21.1371. [PubMed: 15672628]
3. Kakulas BA, Kaelan C. The neuropathological foundations for the restorative neurology of spinal cord injury. Clin Neurol Neurosurg. 2015;129(suppl 1):S1–S7. 10.1016/j.clineuro.2015.01.012. [PubMed: 25683305]
4. Eldahan KC, Rabchevsky AG. Autonomic dysreflexia after spinal cord injury: systemic pathophysiology and methods of management. Auton Neurosci. 2018;209:59–70. [PubMed: 28506502]
5. Fakhoury M Spinal cord injury: overview of experimental approaches used to restore locomotor activity. Rev Neurosci. 2015;26:397–405. [PubMed: 25870961]
6. Gerasimenko Y, Musienko P, Bogacheva I, et al. Propriospinal bypass of the serotonergic system that can facilitate stepping. J Neurosci. 2009;29:5681–5689. 10.1523/JNEUROSCI.6058-08.2009. [PubMed: 19403834]

7. Barthélemy D, Leblond H, Rossignol S. Characteristics and mechanisms of locomotion induced by intraspinal microstimulation and dorsal root stimulation in spinal cats. J Neurophysiol. 2007;97:1986–2000. 10.1152/jn.00818.2006. [PubMed: 17215509]
8. Harnie J, Audet J, Klishko AN, Doelman A, Prilutsky BI, Frigon A. The spinal control of backward locomotion. J Neurosci. 2021;41:630–647. 10.1523/JNEUROSCI.0816-20.2020. [PubMed: 33239399]
9. Marcoux J, Rossignol S. Initiating or blocking locomotion in spinal cats by applying noradrenergic drugs to restricted lumbar spinal segments. J Neurosci. 2000;20:8577–8585. 10.1523/JNEUROSCI.20-22-08577.2000. [PubMed: 11069966]
10. Avelev VD, Mathur R, Behari D, et al. Initiation of locomotion in decerebrate cats by pulsed magnetic fields projected onto spinal cord segments. Neurosci Behav Physi. 2011;41:91–96.
11. Berezovskiĭ VK. The brain stem pathways of locomotion initiation. Article in Russian. Neirofiziologiia. 1991;23:488–505. [PubMed: 1922568]
12. Budakova NN. Stepping movements evoked in a mesencephalic cat by rhythmic stimulation of a dorsal root. Article in Russian. Fiziol Zh SSSR Im I M Sechenova. 1971;57:1632–1640. [PubMed: 5158546]
13. Iwahara T, Atsuta Y, Garcia-Rill E, Skinner RD. Spinal cord stimulation-induced locomotion in the adult cat. Brain Res Bull. 1992;28:99–105. 10.1016/0361-9230(92)90235-p. [PubMed: 1540851]
14. Merkulyeva N, Veshchitskii A, Gorsky O, et al. Distribution of spinal neuronal networks controlling forward and backward locomotion. J Neurosci. 2018;38:4695–4707. 10.1523/JNEUROSCI.2951-17.2018. [PubMed: 29678875]
15. Merkulyeva N, Lyakhovetskii V, Veshchitskii A, Gorskii O, Musienko P. Rostrocaudal distribution of the C-Fos-immunopositive spinal network defined by muscle activity during locomotion. Brain Sci. 2021;11:69. 10.3390/brainsci11010069. [PubMed: 33430215]
16. Lyakhovetskii V, Merkulyeva N, Gorskii O, Musienko P. Simultaneous bidirectional hindlimb locomotion in decerebrate cats. Sci Rep. 2021;11:3252. 10.1038/s41598-021-82722-2. [PubMed: 33547397]
17. Pavlova NV, Bogacheva IN, Bazhenova EYu, Gorsky OV, Moshonkina TR, Gerasimenko YP. Restoration of motor functions in spinal rats by electrical stimulation of the spinal cord and locomotor training. Neurosci Behav Physi. 2020;50:599–606.
18. Minassian K, Jilge B, Rattay F, et al. Stepping-like movements in humans with complete spinal cord injury induced by epidural stimulation of the lumbar cord: electromyographic study of compound muscle action potentials. Spinal Cord. 2004;42:401–416. 10.1038/sj.sc.3101615. [PubMed: 15124000]
19. Gerasimenko YP, Lu DC, Modaber M, et al. Noninvasive reactivation of motor descending control after paralysis. J Neurotrauma. 2015;32:1968–1980. 10.1089/neu.2015.4008. [PubMed: 26077679]
20. Gerasimenko Y, Gorodnichev R, Puhov A, et al. Initiation and modulation of locomotor circuitry output with multisite transcutaneous electrical stimulation of the spinal cord in noninjured humans. J Neurophysiol. 2015;113:834–842. 10.1152/jn.00609.2014. [PubMed: 25376784]
21. Musienko PE, Bogacheva IN, Savochin AA, et al. Non-invasive transcutaneous spinal cord stimulation facilitates locomotor activity in decerebrated and spinal cats. Article in Russian. Ross Fiziol Zh Im I M Sechenova. 2013;99:917–927. [PubMed: 25470942]
22. Malloy DC, Knikou M, Côté MP. Adapting human-based transcutaneous spinal cordstimulation to develop a clinically relevant animal model. J Clin Med. 2022;11:2023. 10.3390/jcm11072023. [PubMed: 35407636]
23. Petruska JC, Barker DF, Garraway SM, et al. Organization of sensory input to the nociceptive-specific cutaneous trunk muscle reflex in rat, an effective experimental system for examining nociception and plasticity. J Comp Neurol. 2014;522:1048–1071. 10.1002/cne.23461. [PubMed: 23983104]
24. Edgerton VR, Gerasimenko Y, Roy RR, Lu DC. Transcutaneous spinal cord stimulation: noninvasive tool for activation of locomotor circuitry. Accessed December 18, 2022. https://patents.google.com/patent/US20170007831A1/en
25. Somers DL, Clemente FR. Transcutaneous electrical nerve stimulation for the management of neuropathic pain: the effects of frequency and electrode position on prevention of allodynia in

a rat model of complex regional pain syndrome type II. Phys Ther. 2006;86:698–709. 10.1093/ptj/86.5.698. [PubMed: 16649893]

26. Havton LA, Christe KL, Edgerton VR, Gad PN. Noninvasive spinal neuromodulation to map and augment lower urinary tract function in rhesus macaques. Exp Neurol. 2019;322:113033. 10.1016/j.expneurol.2019.113033.
27. Shkorbatova P, Lyakhovetskii V, Pavlova N, et al. Mapping of the spinal sensorimotor network by transvertebral and transcutaneous spinal cord stimulation. Front Syst Neurosci. 2020;14:555593. 10.3389/fnsys.2020.555593.
28. Lyakhovetskii V, Shkorbatova P, Gorskii O, Musienko P. [A method for modeling the treatment of patients with motor and visceral disorders in laboratory animals] Patent N2749634 RU. Russian; 2021. Accessed December 18, 2022. https://www.fips.ru/registers-doc-view/fips_servlet?DB=RUPAT&DocNumber=2749634&TypeFile=html
29. Woods JW. Behavior of chronic decerebrate rats. J Neurophysiol. 1964;27:635–644. 10.1152/jn.1964.27.4.635. [PubMed: 14194963]
30. Grill HJ, Norgren R. Neurological tests and behavioral deficits in chronic thalamic and chronic decerebrate rats. Brain Res. 1978;143:299–312. 10.1016/0006-8993(78)90570-x. [PubMed: 630411]
31. Meehan CF, Mayr KA, Manuel M, Nakanishi ST, Whelan PJ. Decerebrate mouse model for studies of the spinal cord circuits. Nat Protoc. 2017;12:732–747. 10.1038/nprot.2017.001. [PubMed: 28277546]
32. Sherrington CS. Flexion-reflex of the limb, crossed extension-reflex, and reflex stepping and standing. J Physiol. 1910;40:28–121. 10.1113/jphysiol.1910.sp001362. [PubMed: 16993027]
33. Fathi Y, Erfanian A. Decoding bilateral hindlimb kinematics from cat spinal signals using three-dimensional convolutional neural network. Front Neurosci. 2022;16: 801818. 10.3389/fnins.2022.801818.
34. Musienko PE, Gorskiĭ OV, Kilimnik VA, et al. Neuronal control of posture and locomotion in decerebrated and spinalized animals. Article in Russian. Ross Fiziol Zh Im I M Sechenova. 2013;99:392–405. [PubMed: 23789442]
35. Hofstoetter US, Freundl B, Binder H, Minassian K. Common neural structures activated by epidural and transcutaneous lumbar spinal cord stimulation: elicitation of posterior root-muscle reflexes. PLoS One. 2018;13:e0192013. 10.1371/journal.pone.0192013.
36. Shkorbatova PY, Lyakhovetskii VA, Merkulyeva NS, et al. Prediction algorithm of the cat spinal segments lengths and positions in relation to the vertebrae. Anat Rec (Hoboken). 2019;302:1628–1637. 10.1002/ar.24054. [PubMed: 30548810]
37. Shapkova EY, Schomburg ED. Two types of motor modulation underlying human stepping evoked by spinal cord electrical stimulation (SCES). Acta Physiol Pharmacol Bulg. 2001;26:155–157. [PubMed: 11695529]
38. Vanderhorst VG, Holstege G. Organization of lumbosacral motoneuronal cell groups innervating hindlimb, pelvic floor, and axial muscles in the cat. J Comp Neurol. 1997;382:46–76. [PubMed: 9136811]
39. Verdugo MR, Rahal SC, Agostinho FS, Govoni VM, Mamprim MJ, Monteiro FO. Kinetic and temporospatial parameters in male and female cats walking over a pressure sensing walkway. BMC Vet Res. 2013;9:129. 10.1186/17466148-9-129. [PubMed: 23803220]
40. Carroll SE, Wiesel SW. Neurologic complications and lumbar laminectomy. A standardized approach to the multiply-operated lumbar spine. Clin Orthop Relat Res. 1992;284:14–23.
41. Li Z, Jiang S, Song X, et al. Collaborative spinal robot system for laminectomy: a preliminary study. Neurosurg Focus. 2022;52:E11:E11. 10.3171/2021.10.FOCUS21499.
42. Edidin AA. Modulating nerves within bone using bone fasteners. Accessed December 18, 2022. https://patents.google.com/patent/US9724151B2/en
43. McCrea DA, Rybak IA. Organization of mammalian locomotor rhythm and pattern generation. Brain Res Rev. 2008;57:134–146. 10.1016/j.brainresrev.2007.08.006. [PubMed: 17936363]
44. Brownstone RM, Wilson JM. Strategies for delineating spinal locomotor rhythm generating networks and the possible role of Hb9 interneurones in rhythmogenesis. Brain Res Rev. 2008;57:64–76. 10.1016/j.brainresrev.2007.06.025. [PubMed: 17905441]

45. Bogacheva IN, Kucher VI, Shcherbakova NA, Musienko Pe, Gerasimenko IuP. Mathematical modeling of the mechanisms of locomotory pattern formation under epidural spinal cord stimulation with consideration of peripheral feedback. Article in Russian. Biofizika. 2005;50:1125–1130. [PubMed: 16358794]
46. Langlet C, Leblond H, Rossignol S. Mid-lumbar segments are needed for the expression of locomotion in chronic spinal cats. J Neurophysiol. 2005;93:2474–2488. 10.1152/jn.00909.2004. [PubMed: 15647400]
47. Gerasimenko Y, Preston C, Zhong H, Roy RR, Edgerton VR, Shah PK. Rostral lumbar segments are the key controllers of hindlimb locomotor rhythmicity in the adult spinal rat. J Neurophysiol. 2019;122:585–600. 10.1152/jn.00810.2018. [PubMed: 30943092]
48. Hägglund M, Dougherty KJ, Borgius L, Itohara S, Iwasato T, Kiehn O. Optogenetic dissection reveals multiple rhythmogenic modules underlying locomotion. Proc Natl Acad Sci U S A. 2013;110:11589–11594. 10.1073/pnas.1304365110. [PubMed: 23798384]
49. Nikitin O, Gerasimenko Yu, Platonov A, Ilieva-Mitutsova L. Features of CPG activation in chronic spinalized cats under spinal cord stimulation. In: Dengler R, Kossev AR, eds. Sensorimotor Control. IOS Press; 2001:172–179.
50. Kato M Chronically isolated lumbar half spinal cord, produced by hemisection and longitudinal myelotomy, generates locomotor activities of the ipsilateral hindlimb of the cat. Neurosci Lett. 1989;98:149–153. 10.1016/0304-3940(89)90501-6. [PubMed: 2710409]
51. Roy FD, Gibson G, Stein RB. Effect of percutaneous stimulation at different spinal levels on the activation of sensory and motor roots. Exp Brain Res. 2012;223:281–289. 10.1007/s00221-012-3258-6. [PubMed: 22990291]
52. Capogrosso M, Wenger N, Raspopovic S, et al. A computational model for epidural electrical stimulation of spinal sensorimotor circuits. J Neurosci. 2013;33:19326–19340. 10.1523/JNEUROSCI.1688-13.2013. [PubMed: 24305828]
53. Komanetsky RM, Padberg AM, Lenke LG, et al. Neurogenic motor evoked potentials: a prospective comparison of stimulation methods in spinal deformity surgery. J Spinal Disord. 1998;11:21–28. [PubMed: 9493766]
54. Wilson-Holden TJ, Padberg AM, Parkinson JD, Bridwell KH, Lenke LG, Bassett GS.A prospective comparison of neurogenic mixed evoked potential stimulation methods: utility of epidural elicitation during posterior spinal surgery. Spine (Phila Pa 1976). 2000;25:2364–2371. 10.1097/00007632-20000915000016. [PubMed: 10984790]
55. Calancie B, Madsen P, Lebwohl N. Stimulus-evoked EMG monitoring during transpedicular lumbosacral spine instrumentation. Initial clinical results. Spine (Phila Pa 1976). 1994;19:2780–2786. 10.1097/00007632-19941215000008. [PubMed: 7899979]
56. Toleikis JR, Skelly JP, Carlvin AO, et al. The usefulness of electrical stimulation for assessing pedicle screw placements. J Spinal Disord. 2000;13:283–289. 10.1097/00002517-200008000-00003. [PubMed: 10941886]
57. Shkorbatova PY, Lyakhovetskii VA, Veshitskii AA, et al. Postnatal growth of the lumbosacral spinal segments in cat: their lengths and positions in relation to vertebrae. Anat Rec (Hoboken). Published online April 24, 2022. 10.1002/ar.24945.

COMMENTS

In this article, Lyakhovetskii et al report interesting results on a novel methodological approach to use transvertebral stimulation to induce locomotor function in the decerebrated cat model. Recent work in the epidural and transcutaneous spinal stimulation fields has shown exciting results demonstrating restoration of motor function in individuals with chronic spinal cord injury. Based on the data presented here, transvertebral stimulation may provide a unique platform to study neuromodulation and motor system physiology that stands at the interface between epidural and transcutaneous stimulation. There is substantial work remaining to evaluate how this technology compares to approaches that have been used clinically. However, the data presented here demonstrates an exciting first step in the development of transvertebral stimulation as a technique to study locomotor function. Jonathan Calvert, PhD Providence, RI, USA

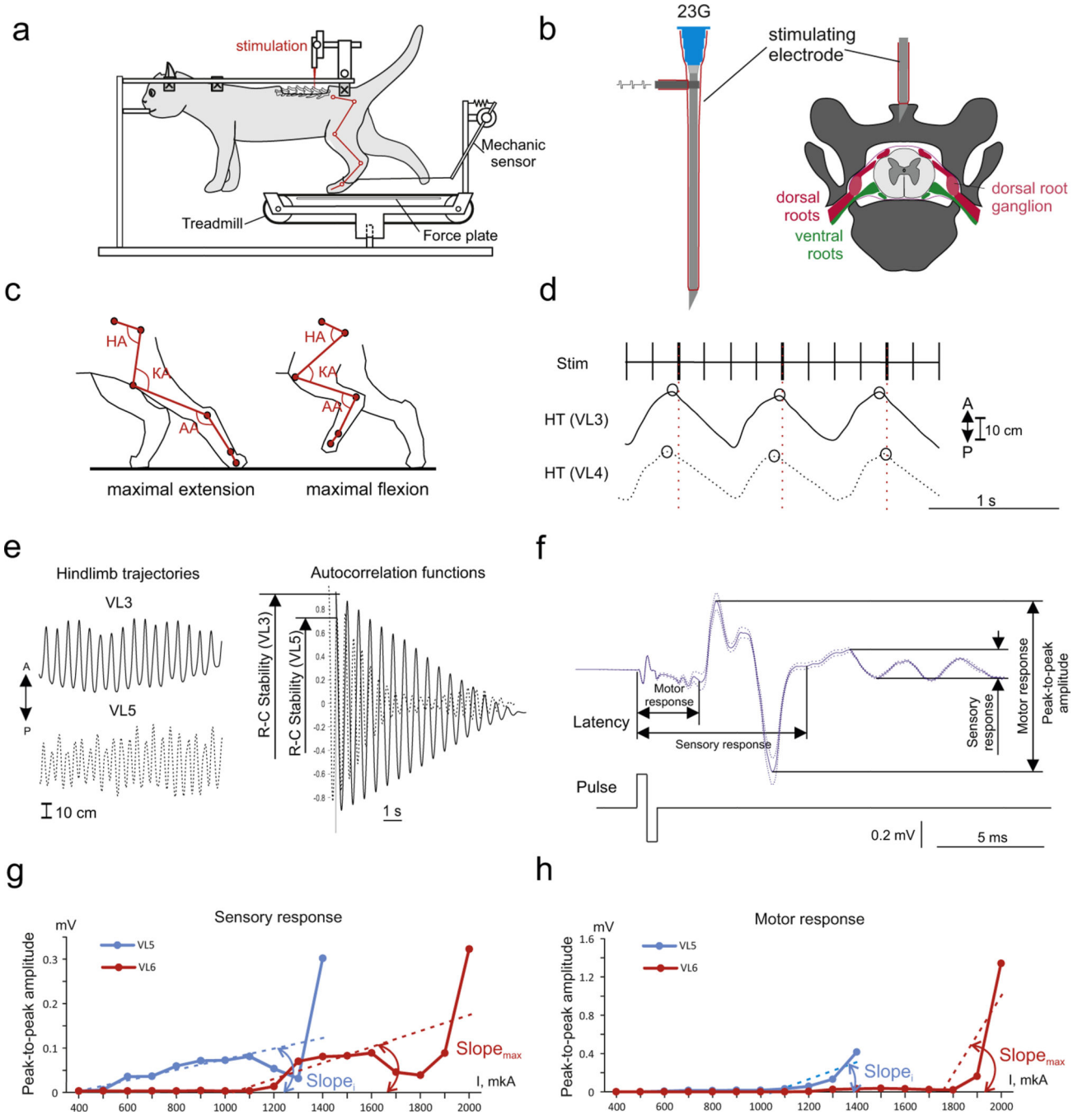

Figure 1.

Experimental setup and methodologic peculiarities. a. Experimental setup. b. The stimulating electrode and its position in the spinous process. c. Angles in the hip (HA), knee (KA), and ankle (AA) joints during maximal extension and maximal flexion of the leg. d. Proximity of hindlimb trajectory (HT) to the multiple of stimulation period. A, anterior; P, posterior. Circles—swing-stance transition point, solid line—left HT of #97 during VL3 stimulation (5 Hz frequency, 0.2-ms pulse duration, 3000-μA current intensity), dotted line—left HT of #97 during VL4 stimulation (5 Hz frequency, 0.2-ms pulse duration,

3000-μA current intensity). e. Rostrocaudal (R-C) stability assessment. Left HTs of #98 during VL3 and VL5 stimulation and their autocorrelation functions (solid line, 3 Hz frequency, 0.2-millisecond pulse duration, 1500-μA current intensity, and dotted line, 3 Hz frequency, 0.2-ms pulse duration, 1800 μA current intensity, respectively). The R-C stability was calculated as the value of the second peak of the autocorrelation function. f. Latencies and peak-to-peak amplitudes assessment (right iliopsoas, VL5 stimulation, #98, mean evoked potential at 1300-μA current intensity). g, h. Slopes assessment at recruitment curves of sensory (G) and motor (H) response (left gastrocnemius lateralis, #99). **Slope**$_{max}$, maximal slope of the given component of evoked potential of given muscle; Slope$_i$, some other slope of the given component of evoked potential of this muscle.

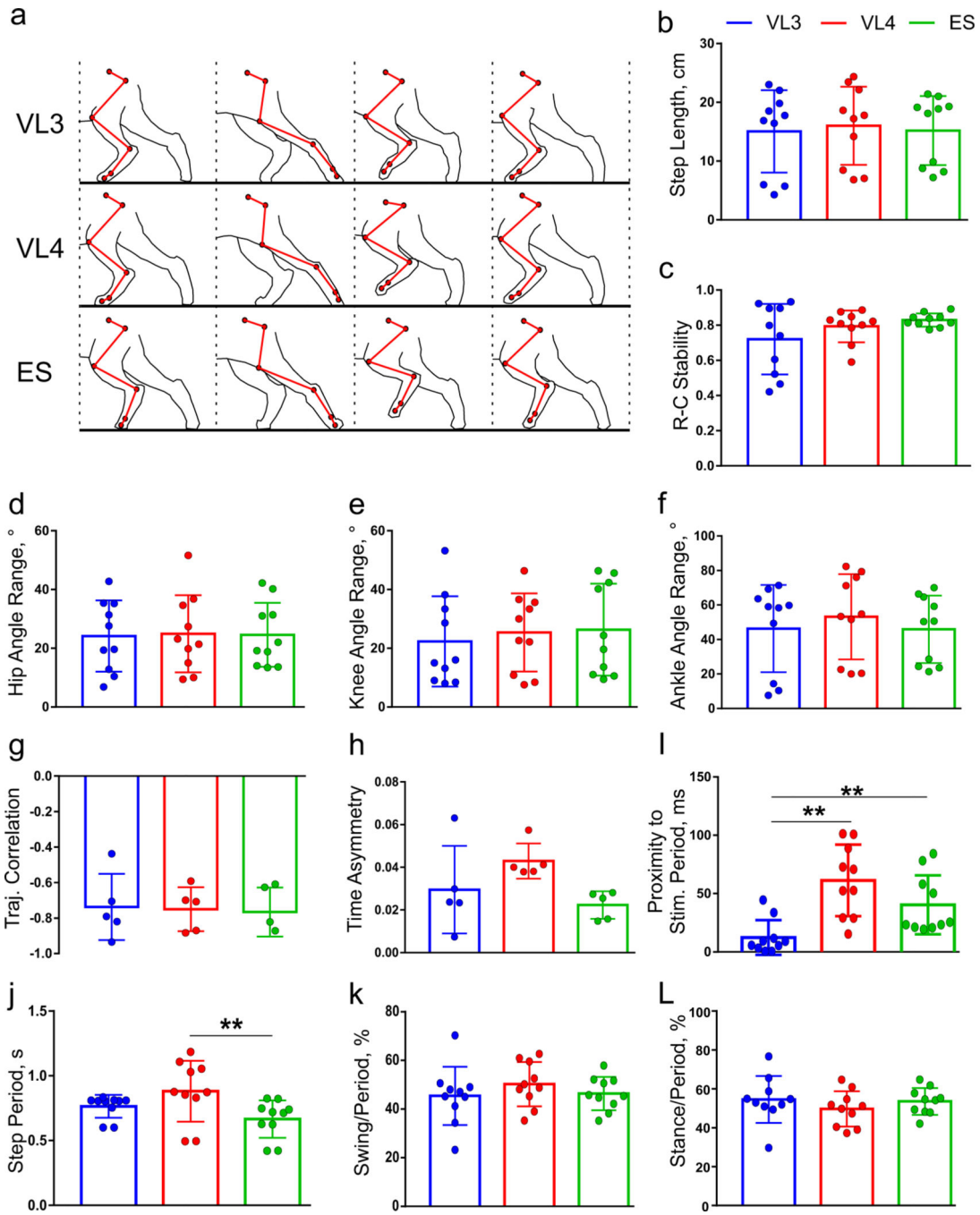

Figure 2.

Parameters for forward walking elicited by transvertebral and epidural stimulation. a. Positions of hindlimbs (start and end of the stance phase, maximal flexion, start of the next stance phase) when stimulation is applied to VL3, VL4, and epidurally. b. Step length (n = 10 hindlimbs). c. Rostrocaudal stability of hindlimb movements (n = 10 hindlimbs). d–f. Angle range in the hip (D), knee (E), and ankle (F) joints (n = 10 hindlimbs). g. Correlation of hindlimb trajectories (n = 5 animals). h. Time asymmetry between hindlimb stepping period (n = 5 animals). i. Proximity of stepping period to a multiple of stimulation period (n

= 10 hindlimbs). j–l. Period of stepping (j), and relative duration of swing (k), and stance (l) phases (n = 10 hindlimbs). Mean ± SD.

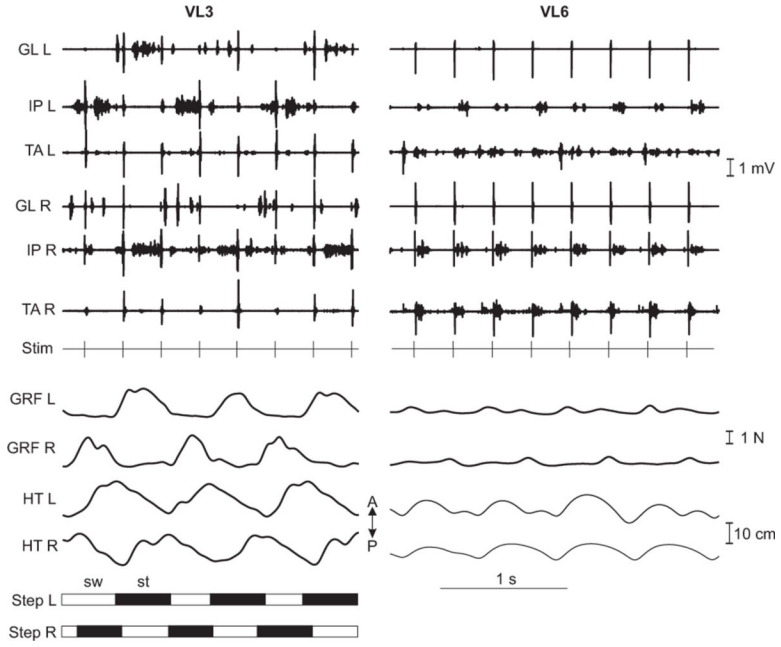

Figure 3.

EMG of muscles, GRF, and trajectories (HT) of both hindlimbs during forward stepping elicited during VL3 stimulation (5-Hz frequency, 0.2-ms pulse duration, 1500-μA current intensity) and VL6 stimulation (5-Hz frequency, 0.2-ms pulse duration, 1100-μA current intensity) of #99. A, anterior; GL, IP, and TA, musculus gastrocnemius lateralis, iliopsoas, and tibialis anterior of left (L) and right (R) hindlimb; P, posterior; st, stance; Step, the phases of hindlimb stepping; Stim, stimulation channel; sw, swing.

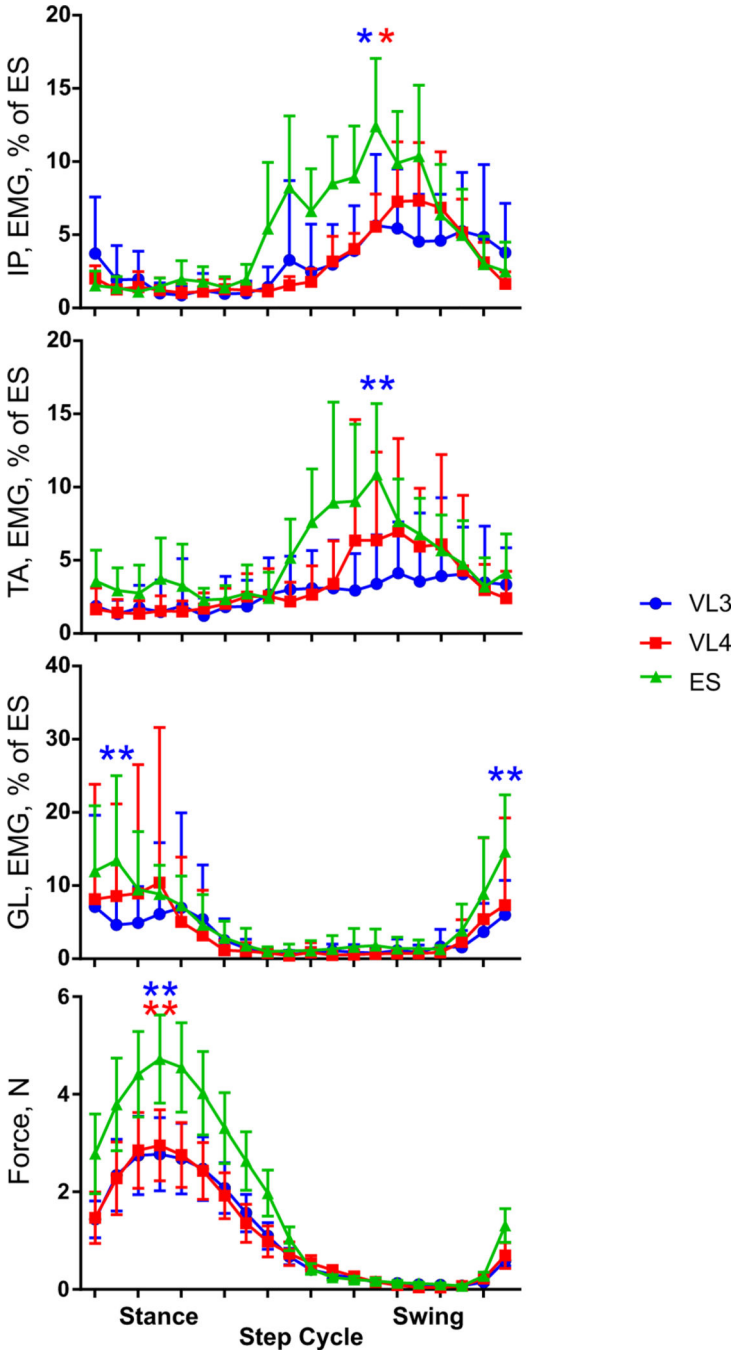

Figure 4.

Mean rectified EMG activity and ground reaction force at the step cycle during the stimulation of VL3, VL4, and ES. EMG activity was normalized per animal basis relative to total EMG activity in the step cycle during ES. $n = 10$ hindlimbs. Mean ± SD. *$p < 0.05$, **$p < 0.01$ relative to VL3 (blue stars) or VL4 (red stars) stimulation.

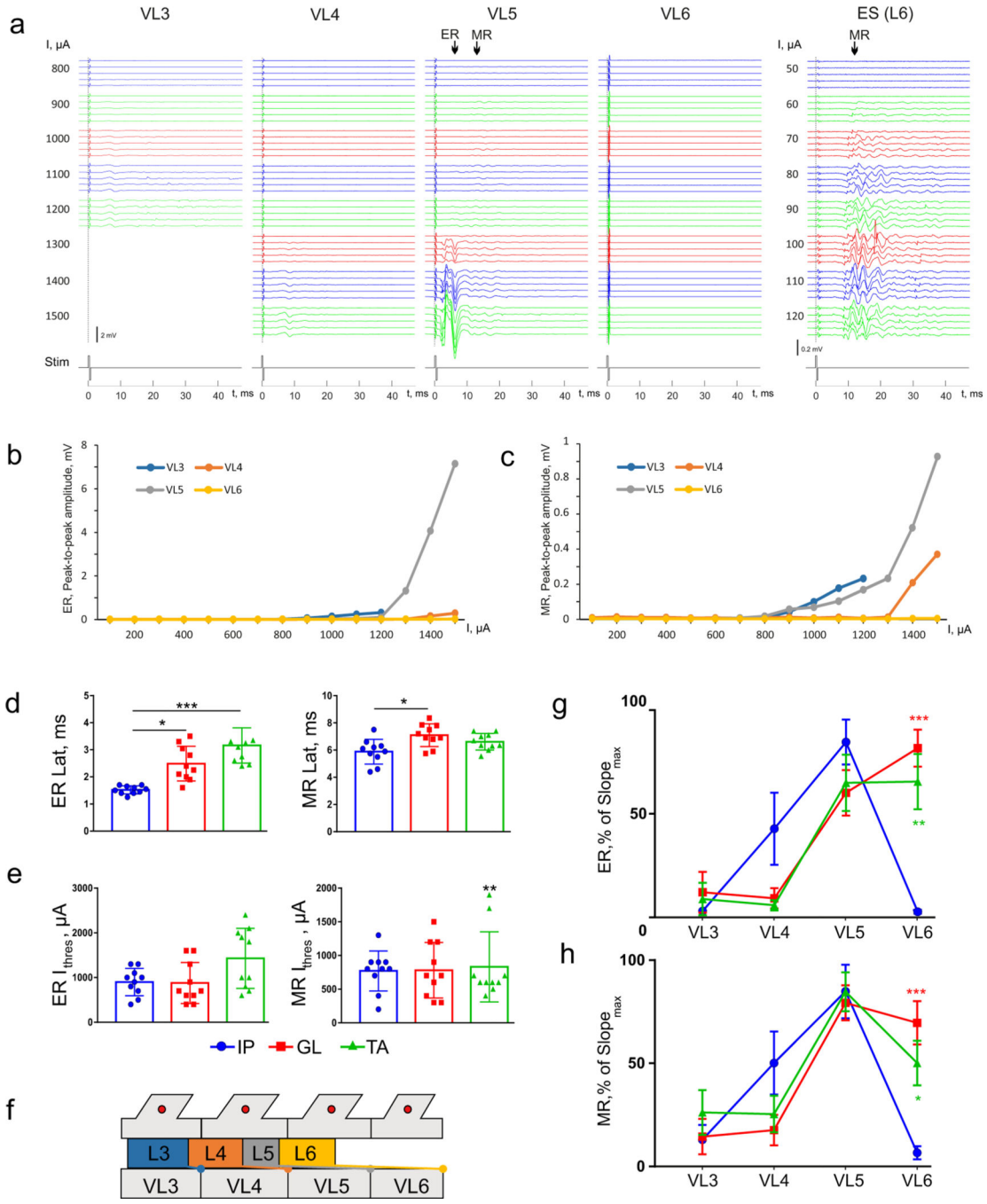

Figure 5.

The evoked potentials in transvertebral stimulation. a–c. The representative example of analysis of the evoked potentials of the right iliopsoas (IP) of #98. a. Evoked potential dynamics with increasing current delivered at VL3–VL6 and during ES of L6 spinal cord segment.Stim, stimulation pulse; ER, early responses; MR, medium responses. Five individual responses are presented at each stimulation current. b, c. Recruitment curves of ER (b) and MR (c) during stimulation of VL3–VL6 vertebrae (mean peak-to-peak amplitude of ten evoked responses in each point). d. ER and MR latencies of musculus IP, GL, and TA

during stimulation in theoptimal for particular muscle vertebra, $n = 10$ hindlimbs, mean±SD. *$p < 0.05$, ***$p < 0.001$. e. Threshold current of ER and MR during stimulation in the optimal for particular muscle vertebra, $n = 10$ hindlimbs, mean ± SD, **$p < 0.01$ relative to the threshold current of TA ER. f. The mean skeletotopy of spinal cord segments in relation to the VL3–VL6 vertebrae (the L3–L6 segments, their roots, and DRGs are marked by different colors corresponding to panels b and c). g, h. Averaged distributions of normalized slopes of ER and MR recruitment curves for IP, GM, and TA during the stimulation of VL3–VL6 vertebrae, $n = 10$ hindlimbs. Mean ± SD. *$p < 0.05$, **$p < 0.01$, ***$p < 0.001$ relative to IP responses.

Table 1.

The Current Used in Different Stimulation Regions to Elicit Locomotion, μA.

	VL2	VL3	VL4		VL5	VL6		ES
Animal\stimulated region				**I, μA**				**Spinal segment**
#97	n/a	3000	700		1100*	3600*	130	L7
#98	1000	1500	3100		1800	2300*	120	L6
#99	3700*	1500	2200		1100*	1100*	100	L6
#102	1900*	700	100		500	1000	20	L6
#104	1500*	600	500		500	2500*	20	L5

n/a, not applicable.

*Inability to elicit the locomotion in this stimulation region using the given current (further increase of current had been ceased because the amplitude of rhythmical synchronous twitching of both hindlimbs became extremely large), VL2–VL6, 2nd–6th–lumbar vertebrae, Spinal segment, the stimulated segment during ES.

Table 2.

Stepping Characteristics When Stimulation is Applied to VL3, VL4, and ES.

Parameter	VL3	VL4	ES	Statistical criterion, FM(3)	*p* Value
Rostrocaudal stability	0.72 ± 0.20	0.79 ± 0.09	0.83 ± 0.04	1.4	0.60
Hip angle range, °	24.14 ±12.12	24.92 ± 13.15	24.58 ± 10.9	0.2	0.97
Knee angle range, °	22.30 ± 15.35	25.36 ± 13.30	26.32 ± 15.65	3.1	0.23
Ankle angle range, °	46.32 ± 25.29	53.18 ± 24.73	45.92 ± 19.52	0.8	0.71
Step length, cm	15.05 ± 7.02	16.01 ± 6.6	15.19 ± 5.87	2.4	0.36
Trajectory correlation	−0.74 ± 0.19	−0.75 ± 0.12	−0.77 ± 0.14	1.2	0.69
Time asymmetry	0.03 ± 0.02	0.04 ± 0.01	0.02 ± 0.01	4.8	0.12
Stepping period, s	0.76 ± 0.09	0.88 ± 0.24	0.67 ± 0.02	12.8	0.0005 *
Swing phase duration, %	45.4 ± 12.0	50.3 ± 9.1	46.4 ± 6.9	4.2	0.14
Stance phase duration, %	54.6 ± 12.1	50.7 ± 9.1	53.6 ± 6.9	4.2	0.14
Proximity to a multiple of the stimulation period	12.73 ± 15.39	63.68 ± 31.91	41.96 ± 26.28	15	0.0001 *

FM, Friedman test with post hoc Dunn's multiple comparison test. Mean ± SD.

* $p < 0.05$.

Table 3.

Parameters of Evoked Potentials During Stimulation in Optimal for Particular Muscle Vertebrae.

Parameter	IP	GL	TA	Statistical criterion, FM(3)	*p* Value
Latency of early responses, ms	1.52 ± 0.15	2.49 ± 0.64	3.16 ± 0.65	17.9	0.0001 *
Latency of medium responses, ms	5.88 ± 0.91	7.09 ± 0.83	6.61 ± 0.61	6.2	0.046 *
Threshold currents of early responses, μA	900 ± 305	880 ± 459	1430 ± 672	5.056	0.09
Threshold currents of medium responses, μA	770 ± 298	780 ±413	830 ± 520	1.59	0.49

FM, Friedman test with post hoc Dunn's multiple comparison test. Mean ± SD.

* $p < 0.05$.